Chapter 9

Fibre-Optic Chemical Sensor Approaches Based on Nanoassembled Thin Films: A Challenge to Future Sensor Technology

Sergiy Korposh, Stephen James, Ralph Tatam and Seung-Woo Lee

Additional information is available at the end of the chapter

http://dx.doi.org/10.5772/53399

1. Introduction

Optical phenomena have been employed extensively by human civilization throughout the centuries for lighting, communication, calculations, observations, etc. and have played a crucial role in industrial development. The applications of the optics increased significantly after the first demonstration of the light guiding phenomenon based on total internal reflection in the 1840s, which was the precursor for the development of modern optical fibres. In modern life, optical fibres found their niche in telecommunications and, more recently, as sensors.

The sensing of chemical compounds is very important for monitoring outdoor and indoor environments (air and soil pollutions and sick building syndrome) [1], diseases (allergy and cancer) [2], and dangerous substances (drugs, hidden bombs, and landmines) [3]. Sensitive, reliable and cheap sensors for application in different areas of human activities are still sought.

Optical fibre-based measurement techniques have attracted a great deal of attention in a variety of analytical areas such as chemical and biological sensing, environmental monitoring and medical diagnosis. The variety of different designs and measurement schemes that may be employed using optical fibres provides the potential to create very sensitive and selective measurement techniques in real environments.

Different approaches exist for creation of fibre-optic sensors (FOS), which generally can be classified into two groups depending on the sensing mechanism: intrinsic and extrinsic fibre-optic sensors [4]. Interferometric sensors can be made that respond to an external stimulus by a change in the optical path length and thus a phase difference in the interferometer. Tradi-

tional interferometers such as Michelson, Mach Zehnder [5, 6, 7], Fizeau, Sagnac [8] and Fabry Perot [9, 10, 11] used for measuring of both chemical and physical parameters can be constructed utilizing optical fibres.

Fibre-optic sensors based on the evanescent wave absorption effect are an example of simple, cost effective yet very efficient type of intrinsic fibre-optic sensor [12]. As light travels along the core of the optical fibre, a small portion of energy penetrates the cladding in the form of an *evanescent wave*, the intensity of which decays exponentially with the distance from the interface between the cladding and the surrounding environment. Typically the penetration depth of evanescent wave into surrounding medium is in order of hundreds of nanometers.

This allows the direct analysis of the spectroscopy of an analyte in contact with the surface of the optical fibre. Alternatively an indirect measurement approach can be employed, whereby a chemically sensitive functional coating, which changes its optical properties when it comes into contact with the analyte, can be deposited onto the surface of the optical fibre. Analysis of the transmission spectrum can provide quantitative and qualitative information on the chemical species under examination. The use of chemically sensitive coatings means that the operating wavelength of the sensor is defined by the coating properties, rather than the absorption spectrum of the analyte, which can be advantageous. Fibre optic sensors based on the intrinsic evanescent wave offer the prospect for the development of cheap and compact devices, due to combination of low cost light emitting diodes (LED) and photodetectors. The sensitivity of the device is dependent on the length of the sensing area and for efficient operation coating materials with the strong absorption features should be selected. Generally, the simplest implementation of the fibre optic evanescent wave spectroscopy is application of the multimode optical fibre with the silica core and plastic cladding. The plastic cladding can easily be removed to allow the access to the evanescent wave and replaced with the functional coating providing sensor with its sensitivity and selectivity. In the case of the singlemode fibres with silica core and silica cladding polishing, etching or tapering is employed in order to get an access to the evanescent wave.

Intrinsic FOS allows to implement different measurements designs within an optical fibre based on the gratings (Bragg Gratings, FBG and long period gratings, LPG) written into the fibre core in which the changes in the reflected light due to changes in the grating period is measured to detect the effect caused by an external stimulus [13, 14]. Refractometers and chemical sensors based on optical fibre gratings, both FBGs and LPGs, have been extensively employed for refractive index measurements and monitoring associate chemical processes since they offer wavelength-encoded information, which overcomes the referencing issues associated with intensity based approaches.

Among the optical waveguide devices that have been investigated, tapered optical fibre sensors are able to measure environmental parameters (refractive index, chemical concentration, etc.) with high sensitivity owing to the large proportion of the energy of the propagating mode extending into the surrounding environment in the form of an evanescent field [15, 16, 17]. The tapered area of the optical fibre facilitates evanescent wave spectroscopy, in which the absorption spectrum of the surrounding medium is measured. Alternatively, the influence

http://dx.doi.org/10.5772/53399

of the surrounding medium on the properties of the optical modes of the tapered waveguide can be explained as a change in the refractive index, i.e. it will operate as a refractometer.

Various deposition techniques, such as dip- and spin-coatings, layer-by-layer deposition (LbL) electrostatic self-assembly, Langmuir-Blodgett deposition, and chemical and physical vapour deposition have been employed for the functional coating of optical fibres. Among these techniques, the LbL technique, which is based on the alternate adsorption of polycations and polyanions onto the surface, has been used as a powerful surface modification method. This alternate adsorption technique is still expanding its potential because of its versatility and convenience for the fabrication of nano-assembled thin films employing various organic and inorganic materials.

In this chapter we will describe recent approaches to the development of fibre-optic chemical sensors utilising different measurement designs based on evanescent wave, tapered and long period gratings functionalized with nanoassembled thin films. Advantages and characteristic features of each measurement design will be discussed and examples of the sensitive and selective detection of various chemical analytes will be demonstrated. In addition, the potential of fibre-optic chemical sensors for future sensor technology will be discussed.

2. Fibre-optic chemical sensor designs

2.1. Evanescent wave fiber-optic sensor

To fabricate the evanescent wave fibre-optic sensor (EWFOS), a short section of the plastic cladding of a multimode optical fibre (HCS silica core/plastic cladding with 200 μm core diameter, Ocean Optics) was replaced with a functional coating of alternate poly(diallyldimethylammonium chloride) (PDDA, Mw: 200000–350000, 20 wt% in H_2O) and tetrakis-(4-sulfophenyl)porphine (TSPP, M_w=934.99) layers, Scheme 1. A schematic illustration of this method is shown in Figure 1a [18]. Before assembly, the previously stripped section of the optical fibre was cleaned with concentrated sulfuric acid (96%), rinsed several times with deionized water, and treated with 1 wt% ethanolic KOH (ethanol/water = 3:2, v/v) for about 10 min with sonication in order to functionalize the surface of the silica core with OH groups. The fibre core was then rinsed with deionized water, and dried by flushing with dry nitrogen gas. The film was prepared by the alternate deposition of PDDA (5 mg mL^{-1} in water) and TSPP (1 mM in water) (where one cycle is considered to be a combined PDDA/TSPP bilayer) by introducing a coating solution (150 μL) into the deposition cell with intermediate processes of water washing and drying by flushing with nitrogen gas being undertaken between the application of layers. In every case, the outermost surface of the alternate film was TSPP. The film is denoted by $(PDDA/TSPP)_x$, where x indicates the number of adsorption cycles.

The measurement principle of the device is based on the analyte-induced optical change in the transmission spectrum of the coated optical fibre.

The penetration depth (d_p) of the evanescent wave is described by [4]:

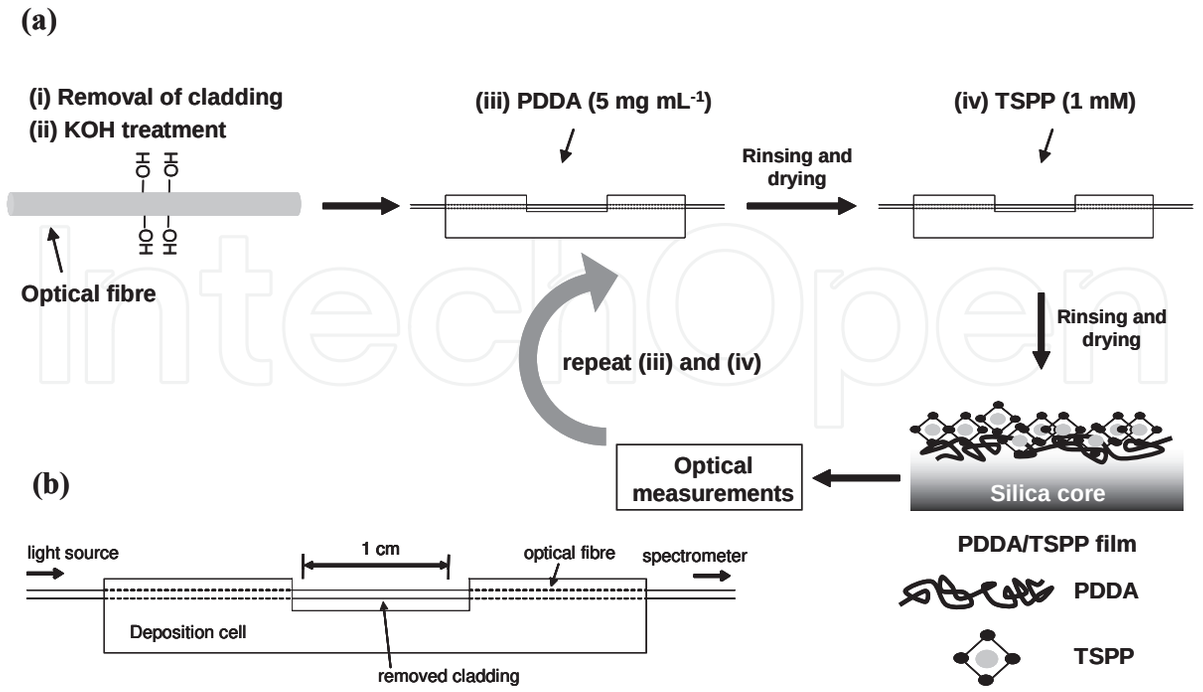

Figure 1. (a) Schematic illustration of the layer-by-layer adsorption of TSPP and PDDA on a multimode optical fibre and (b) deposition cell used for optical fibre coating [18].

$$d_p = \frac{\lambda}{2\pi(n_{eff}^2 - n_c^{\,2})^{1/2}} \tag{1}$$

where λ is the wavelength of light in free space, n_c is the refractive index of the cladding and n_{eff} is the effective refractive index of the mode guided by the optical fibre.

Porphyrin compounds can be used as a sensitive element for optical sensors because their optical properties (absorbance and fluorescence features) depends on the environmental conditions in which molecule is present [20]. Porphyrins are tetrapyrrolic pigments that widely occur in nature and play an important role in many biological systems [21]. The optical spectrum of the solid state porphyrin is modified as compared to that of porphyrin in solution, due to the presence of strong $\pi-\pi$ interactions [22]. Interactions with other chemical species can produce further optical spectral changes, thus creating the possibility that they can be applied to optical sensor systems. The high extinction coefficient (> 200,000 cm^{-1}/M) makes porphyrin especially attractive for the creation of optical sensors.

2.2. Tapered fiber-optic sensor

A tapered optical fibre may be fabricated by simultaneously heating and stretching a short section of a single mode optical fibre. This creates a region of fibre with reduced and uniform diameter (the waist) that is bounded by conical sections where the diameter of the fibre changes

http://dx.doi.org/10.5772/53399

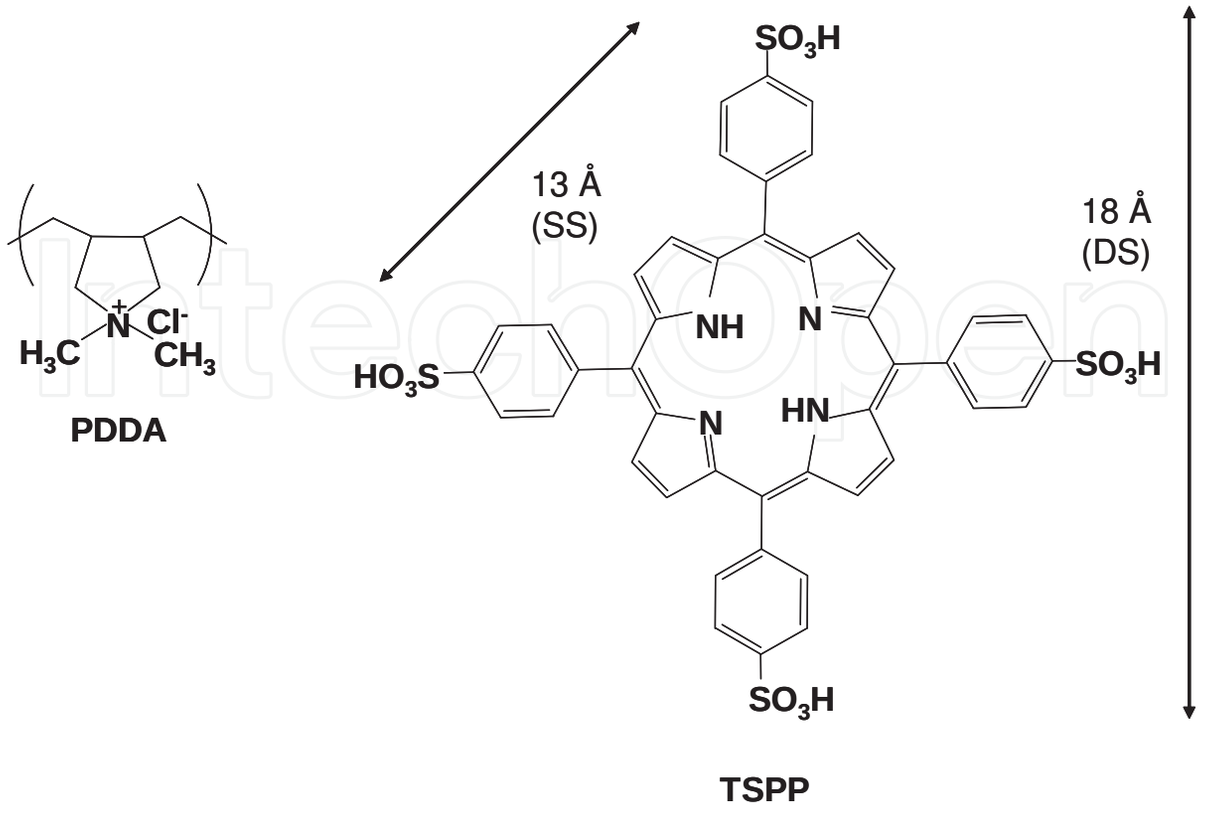

Scheme 1. Structural models of the polycation (PDDA) and porphyrin (TSPP) compounds used for sensor fabrication [19]: SS, side length of square; DS, diagonal length of square.

to merge the tapered section with the unperturbed surrounding single mode fibre. The optical properties of the tapered fibre waveguide are influenced by the profile of the conical tapering sections, by the diameter of the taper waist and by the optical thickness of the surrounding medium. The proportion of the power in the evanescent field, and thus the interaction with the surrounding medium, increases with decreasing diameter of the taper waist [23, 24]. In the tapering section, the guided mode of the single mode fibre is converted into a mode of the waist, Figure 2. In adiabatic tapers this is achieved without coupling to higher order modes. In non-adiabatic tapers the taper profile is such that a proportion of the light is coupled into higher order modes of the tapered section, which interfere to produce the channeled spectra reported for tapers of diameter of order 5 μm [23, 25].

The detailed description of the fibre tapering procedure can be found elsewhere [23]. Briefly, a single mode silica optical fibre was tapered using the heat and pull technique. Firstly, the polymer buffer coating was removed from a 50 mm long section in the middle of a ~1 m length of the single mode optical fibre using a mechanical stripper. The stripped section of the optical fibre was then fixed on a 3-axis flexure stage (NanoMax™, Thorlabs) and exposed to the flame produced by a gas burner (max temperature 1800°C) for approximately 60 sec while the ends of the fibre were pulled in opposite directions using translation stages. Nonadiabatic optical fibre tapers of diameters 9, 10 and 12 μm, all having a taper waist of length 20 mm, were

fabricated. The dimensions of the tapers were determined using a digital optical microscope, DZ3 Union Optical Co., Ltd., Japan.

The LbL method described above has been used to deposit a multilayer porphyrin film over the tapered region of a single mode optical fibre with the aim of demonstrating a gas sensor, Figure 2a. The effect of the polycation on the optical properties and structure of the multilayer porphyrin film was studied thoroughly. It is suggested that, by using poly(allylamine hydrochloride) (PAH, M_r: 56000) for the porphyrin film preparation instead of PDDA, the form of the aggregation of the TSPP is modified and provides improved optical properties that facilitate the detection of wider class of chemicals. Moreover the analyte-induced refractive index change of the prepared multilayer porphyrin film was monitored using tapered optical fibres.

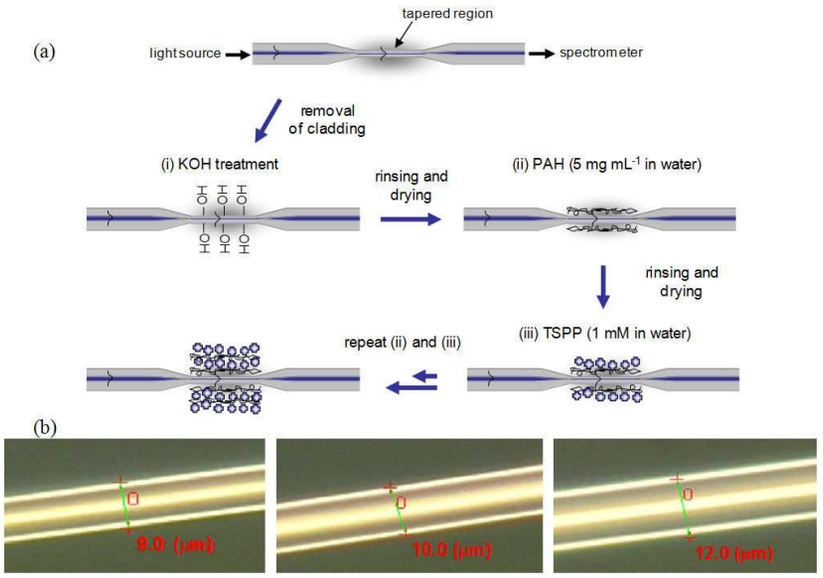

Figure 2. (a) Schematic illustration of the layer-by-layer adsorption of TSPP and PAH on a tapered optical fibre and (b) optical images of the tapered region of the optical fibres with different waist diameter.

2.3. Optical fibre long period gratings

LPGs promote coupling between the propagating core mode and co-propagating cladding modes, i.e. work as transmission gratings. The high attenuation of the cladding modes results in the transmission spectrum of the fibre containing a series of resonance bands centred at discrete wavelengths, each resonance band corresponding to coupling to a different cladding mode, as shown in Figure 3 [26].

The refractive index sensitivity of LPGs arises from the dependence of the phase matching condition upon the effective refractive index of the cladding modes, which is governed by Equation 2 [26]:

http://dx.doi.org/10.5772/53399

$$\lambda_{(x)} = (n_{core} - n_{clad(x)})\Lambda \quad (2)$$

where $\lambda_{(x)}$ represents the wavelength at which the coupling occurs to the linear polarized (LP_{0x}) mode, n_{core} is the effective RI of the mode propagating in the core, $n_{clad(x)}$ is the effective RI of the LP_{0x} cladding mode, and Λ is the period of the grating. The modes to which coupling occurs is dependent upon the period of the grating, and this has a significant influence on the form of the transmission spectrum, as is clear from Figure 3.

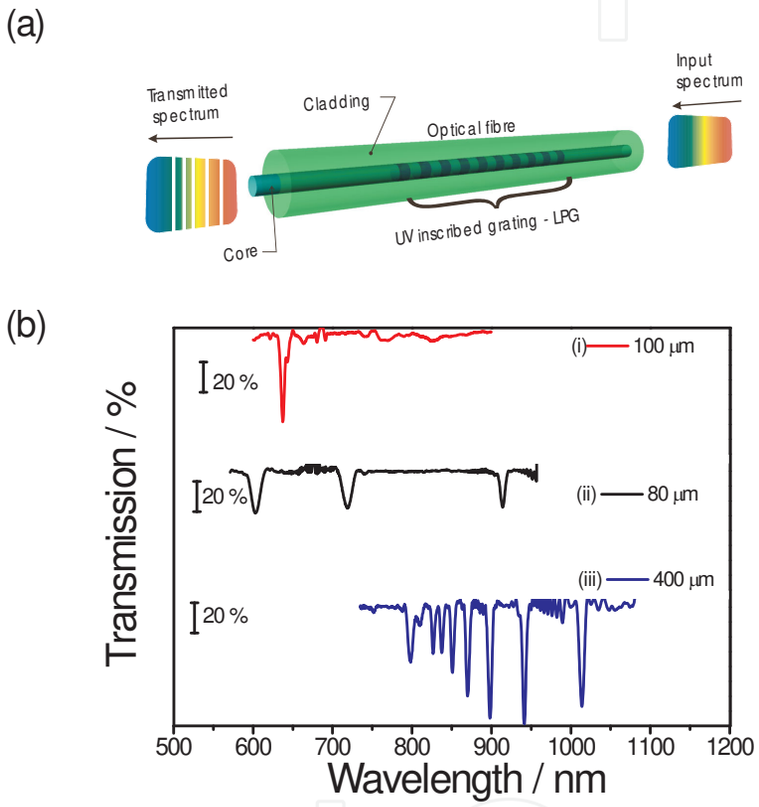

Figure 3. (a) Schematic illustration of the LPG structure and (b) transmission spectra of LPGs with different grating periods fabricated in an optical fibre of cut-off wavelength 670 nm (Fibrecore SM750): (i) 80 µm, (ii) 100 µm, and (iii) 400 µm [27].

The effective indices of the cladding modes are dependent upon the difference between the refractive index of the cladding and that of the medium surrounding the cladding. The highest sensitivity is shown for surrounding refractive indices close to that of the cladding of the optical fibre, provided that the cladding has the higher refractive index [28]. For surrounding refractive indices higher than that of the cladding, the centre wavelengths of the resonance bands show a considerably reduced sensitivity [29].

A detailed description and reference to the optical properties of LPGs can be found elsewhere [27, 30, 31]. In this work, an LPG of length 30 mm with a period of 100 µm was fabricated in a

single mode optical fibre (Fibercore SM750) with a cut-off wavelength of 670 nm using point-by-point UV writing process. The photosensitivity of the fibre was enhanced by pressurizing it in hydrogen for a period of 2 weeks at 150 bar at room temperature.

The coated LPG was used for the detection of ammonia in the gas phase and in solution. For the detection of ammonia in solution, the LPG was coated with mesoporous PDDA/SiO_2 nanoparticles (NPs) (SNOWTEX 20L (40–50 nm), Nissan Chemical) film using the LbL process and infused with functional compound, TSPP, as illustrated in Figure 4a. As the LPG transmission spectrum is known to be sensitive to bending, for the film deposition process and ammonia detection experiments the optical fibre containing LPG was fixed within a special holder, as shown in Figure 4b, such that the section of the fibre containing the LPG was taut and straight throughout the experiments [30]. The detailed procedure of the deposition of the SiO_2 NPs onto the LPG and infusion of the TSPP compound has been reported previously [27]. Briefly, the section of the optical fibre containing LPG, with its surface treated such that it was terminated with OH groups, was alternately immersed into a 0.5 wt% solution containing a positively charged polymer, PDDA, and, after washing, into a 1 wt% solution containing the negatively charged SiO_2 NPs solution, each for 20 min. This process was repeated until the required coating thickness was achieved. When the required film thickness had been achieved (i.e. when the development of the second resonance band was observed with the fibre immersed into water), ca. after 10 deposition cycles, the coated fibre was immersed in a solution of TSPP as functional compound for 2 h, which was infused into the porous coating and provided the sensor with its specificity. Due to the electronegative sulfonic groups present in the TSPP compound, an electrostatic interaction occurs between TSPP and positively charged PDDA in the PDDA/SiO_2 film. After immersion into the TSPP solution, the fibre was rinsed in distilled water, in order to remove physically adsorbed compounds, and dried by flushing with N_2 gas. The compounds remaining in the porous silica structure were bound to the surface of the polymer layer that coated each nanosphere. This effectively increased the available surface area for the compounds to bond to. The presence of functional chemical compounds increased the RI of the porous coating and resulted in a significant change in the LPG's transmission spectrum, consistent with previous observations for increasing the coating thickness [32]. All experiments have been conducted at 25°C and 50% of rH.

For the ammonia detection in gas phase the LPG was designed to operate at the phase match turning point. In coated LPGs, for coupling to a particular cladding mode, the phase matching turning point occurs at a specific combination of grating-period and optical thickness of the coating. Near the phase matching turning point conditions, it is possible to couple to the cladding mode at two different wavelengths, with the corresponding resonance band wavelengths showing opposite sensitivity to perturbations to the properties of the coating [33]. LPGs show there highest sensitivity to environmental perturbations when operating in this regime [33]. The LPG was coated with an alternate thin film composed of poly(acrylic acid) (PAA, M_w:4000000) and PDDA, Figure 5. PAA is a promising candidate for the creation of ammonia sensors, of which free carboxylic acid groups lead to the high sensitivity and selectivity toward amine compounds [34]. Recently, we have reported a quartz crystal microbalance (QCM) gas sensor based on the alternate deposition of TiO_2 and PAA for the sensitive detection of amine

http://dx.doi.org/10.5772/53399

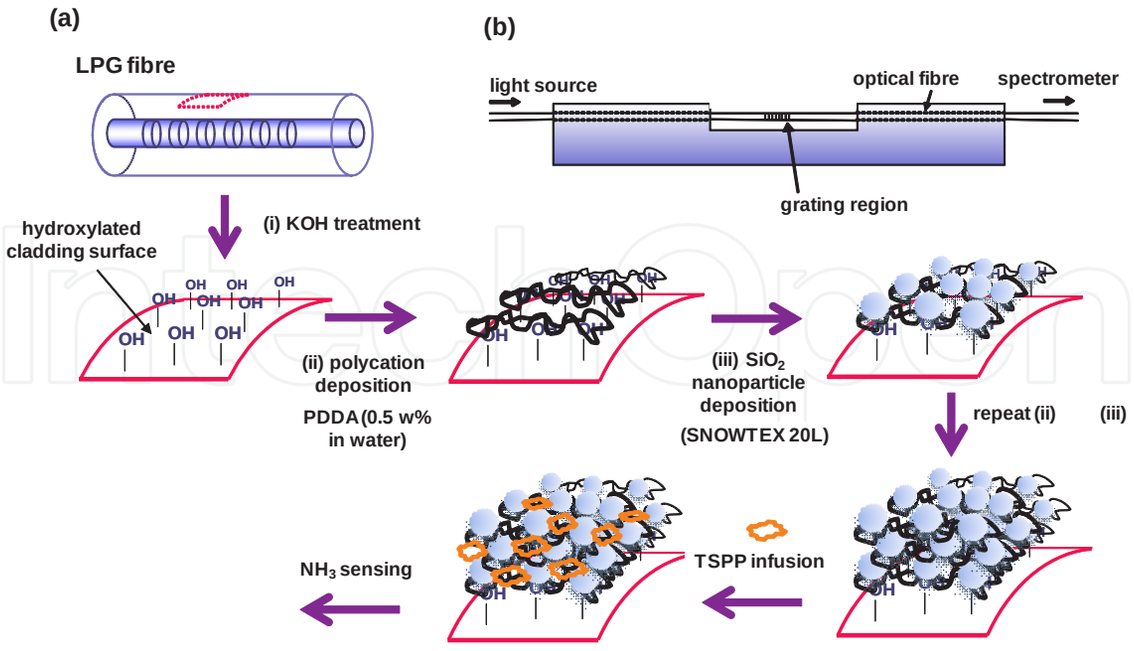

Figure 4. (a) Schematic illustration of the electrostatic self-assembly deposition process and (b) deposition cell with a fixed LPG fibre.

odors. However, QCM sensors still have a weakness that the sensor response can be easily affected by humidity [35]. The current approach would enable the LPG sensor performance based on the acid-base interaction of amine odors to the COOH moiety of PAA under humid conditions.

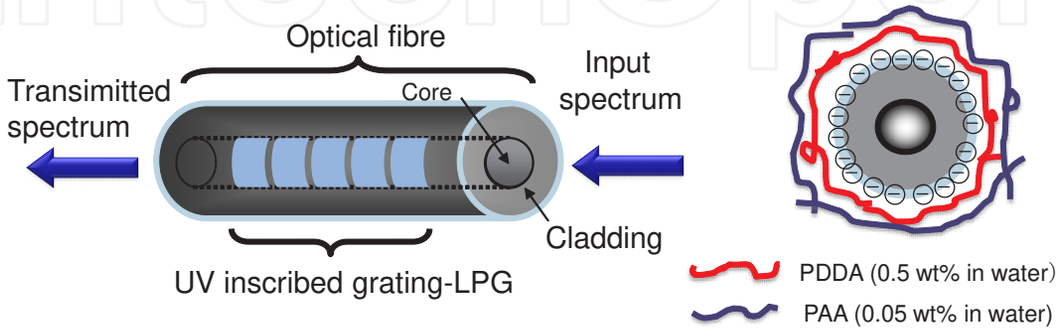

Figure 5. (a) Schemetic illustration of an LPG and its surface modification using PDDA and PAA [34].

3. Sensing approaches

3.1. Sensing based on evanescent wave fiber-optic sensors

Ammonia is one of the major metabolic compounds and the importance of its detection has been recently emphasized because of its correlation with specific diseases [36,37]. At normal physiological conditions ammonia can be expelled from the slightly alkaline blood and emanated through the skin or exhaled with the breath. Dysfunction in the kidneys or liver that converts ammonia to urea can result in an increase of the ammonia concentration in breath or urine. Consequently, the detection of the ammonia gas present in the breath or urine can be used for the early diagnostics of liver or stomach diseases [36].

Ammonia-induced changes in the transmission spectrum of the $(PDDA/TSPP)_5$ film are shown in Figure 6. As ammonia concentration increased from 0 to 20 ppm, a concomitant intensity change is observed at several wavelengths; at 706 nm the intensity increases, whereas at 350 and 470 nm it decreases. Upon exposure of the $(PDDA/TSPP)_5$ film to ammonia, the largest intensity change was observed at 706 nm. The interaction between ammonia and TSPP molecules leads to the deprotonation from the pyrolle ring and hence affects the interaction between TSPP molecules. Similarly, the largest change in absorbance is observed at 706 nm (Q band), which is attributed to the aggregation structure of TSPP [38]. The difference spectra were obtained by subtracting a spectrum measured in ammonia atmosphere from a spectrum measured in air.

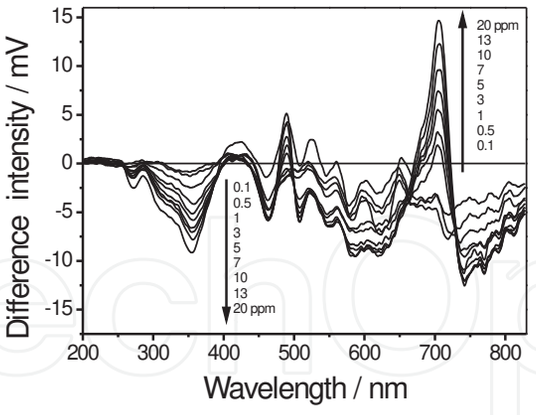

Figure 6. Optical transmission difference spectra of the optical fibre coated with a five-cycle PDDA/TSPP alternate film on exposure to ammonia concentrations ranging from 0–20 ppm.

The dynamic response of the $(PDDA/TSPP)_5$ coated fibre to exposure to ammonia was monitored at 350, 470 and 706 nm (Figure 7a). As can be seen from the result, the sensor response is fully reversible for low ammonia concentrations (up to 1 ppm). However, at higher concentrations the sensor takes a longer time to return to the base line. The base line may be recovered by flushing with air for sufficient time, as shown in Figure 7a. Alternatively, the

http://dx.doi.org/10.5772/53399

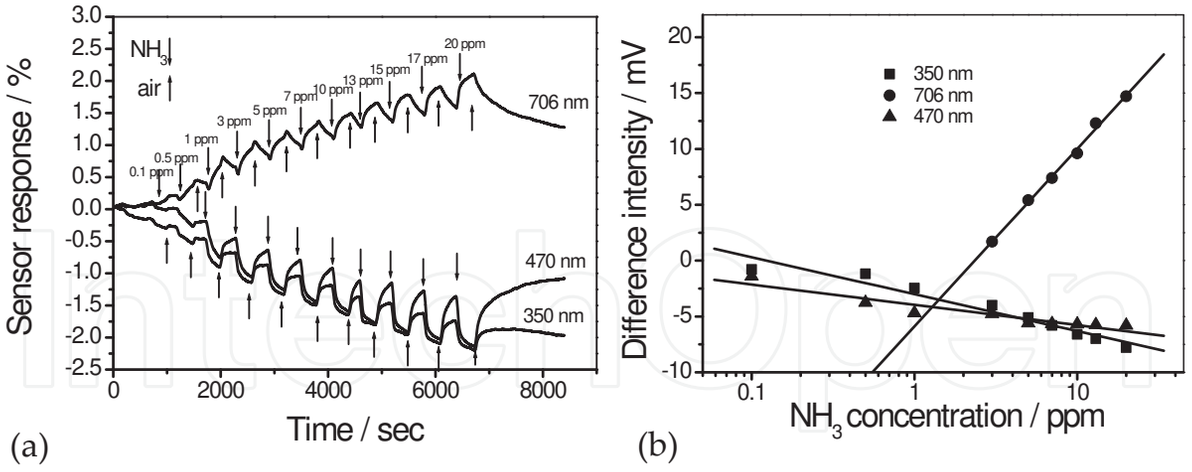

Figure 7. (a) Dynamic response of the optical fibre coated with a five-cycle PDDA/TSPP alternate film for ammonia concentrations ranging from 0–20 ppm at 350, 470, and 706 nm. (b) Calibration curves at 350 nm (squares), 470 nm (rhombuses), and 706 nm (circles). Lines show the linear fitting and are used only as guidance to an eye.

sensor response can be regenerated by rinsing for a few seconds in distilled water [39]. The calibration curve at each wavelength was plotted from the recorded spectra at given ammonia concentrations. The sensor shows linear responses at all wavelengths for a wide concentration range from 0.1 to 20 ppm and the highest sensitivity was observed at 706 nm (Figure 7b).

The response and recovery times (t_{90}) of the sensor to increasing ammonia concentration were within 1.6-2.5 min and 1.8-3.2 min, respectively (see Figure 7a). The sensitivity of the sensor depends on the wavelength and has different directions; for 350 and 470 nm, it is negative, and for 706 nm it is positive. The highest sensitivity was measured at 706 nm, corresponding to the optical change of the Q band of TSPP. The current sensor system has a limit of detection (*LOD*) of 0.9 ppm. The limit of detection was defined according to:

$$LOD = 3s / m \tag{3}$$

where $\sigma \approx 0.31$ is the standard deviation, and m is the slope ($\Delta I/\Delta c$) of the calibration curve, where c is the ammonia concentration and I is the measured intensity (mV) [40].

The results suggest that it will be possible to create a low-cost fibre optic sensor by selecting a LED and a photodiode with parameters that coincide with the wavelength at which the largest ammonia-induced changes were observed (706 nm).

The optical fibre acts as a platform that may be exploited to facilitate the detection of different chemicals by coating the fibre with appropriate functional materials. In order to demonstrate its capability, it was employed for the detection of the gaseous compounds excreted from the human body. Gaseous compounds excreted from the human body are believed to reflect certain metabolic conditions of the organism as well as the blood gaseous content [41]. A lot of information about human skin excretion is present in the literature. In gas chromatography

(GC) based experiments, variety of compounds were found to be emitted by human skin, such as acetone [42], ammonia [43], hydrocarbons [44] and aromatics [45], and the quantity of some of these compounds was correlated to blood content. Ammonia gas has been known to emanate through the skin from serum and its level depends on the humans health conditions [37]. Studies have demonstrated the possibility of identifying human subjects through the examinations of their volatile organic compound (VOC) odour patterns, formulating the idea of personal "smellprint" as an analogue of the fingerprint [46]. Applicability of electronic nose techniques was shown for the classification of bacteria related to human diseases [47,48], urinary tract infections [49] and further progress to metabolic disorders such as diabetes [50] or renal dysfunction [51]. The detection of renal failure in rats [52] and of lung cancer in people [53] was achieved using the breath sniffing method by arrays consisting of appropriately modified chemiresistors. Analysis of gases emitted from skin, however, is mainly being performed with the use of GC, which in spite of its high sensitivity and selectivity is expensive and time-consuming and requires a well- trained operator. Development of miniaturized sensing devices is expected to overcome the drawbacks of conventional approaches.

Here, a preliminary study of an optical fibre based skin gas sensor is discussed.The measurement setup for the skin gas analysis is shown in Figure 8. One end of the optical fibre was connected to a deuterium/halogen tungsten light source (DH-2000-BAL, Micropack) and other end was connected to an optical spectrometer (S1024DW, Ocean Optics) via fibre-optic connectors. The fabricated optical sensor was located inside a small acryl sensing cell (cylinder shape with radius r=3.5 cm, height h=1 cm, volume V=38.5 cm^3) containing a humidity and temperature recording logger (Hygrochron, KN Laboratories: RH range of 0–95%; accuracy ±5% at 25 ^oC in the range of 20–80% RH and reading resolution 0.1%).

For skin gas measurements, the top of the acryl cell was completely covered by palm surface. The optical measurement of palm skin emanations inside the chamber was done for 5-30min while the optical output spectrum and optical changes at selected wavelengths were recorded every second using an Ocean Optics software (OOIBase32).

To test the influence of the humidity, the acryl sensing chamber was additionally connected to a humidified air generating system through the additional inlet and outlet of the measuring cell, as shown in Figure 8. Dry compressed air was divided into two flows by the use of flow controllers (FC1 and FC2) and one of the flows passed through a bubbling bottle with deionized water to humidify the air. Recombination of the flows of dry and wet air was used to obtain the different levels of relative humidity.

Sensor response to changes in relative humidity was measured every second by recording the transmission spectrum of the optical fibre coated with a thin film. To explore the reproducibility of the measurements, the response of the fibre optic sensor was recorded twice at three different levels of humidity and flushed with dry air between each measurement.

The sensor response to palm skin gas was assessed by recording the changes of the optical properties of a $(PAH/TSPP)_{10}$ film deposited on the optical fibre. Optical spectral changes induced by the presence of the skin gases emitted from two different people (R and S) are shown in Figure 9a (spectral change) and Figure 9b (dynamic intensity change at selected

http://dx.doi.org/10.5772/53399

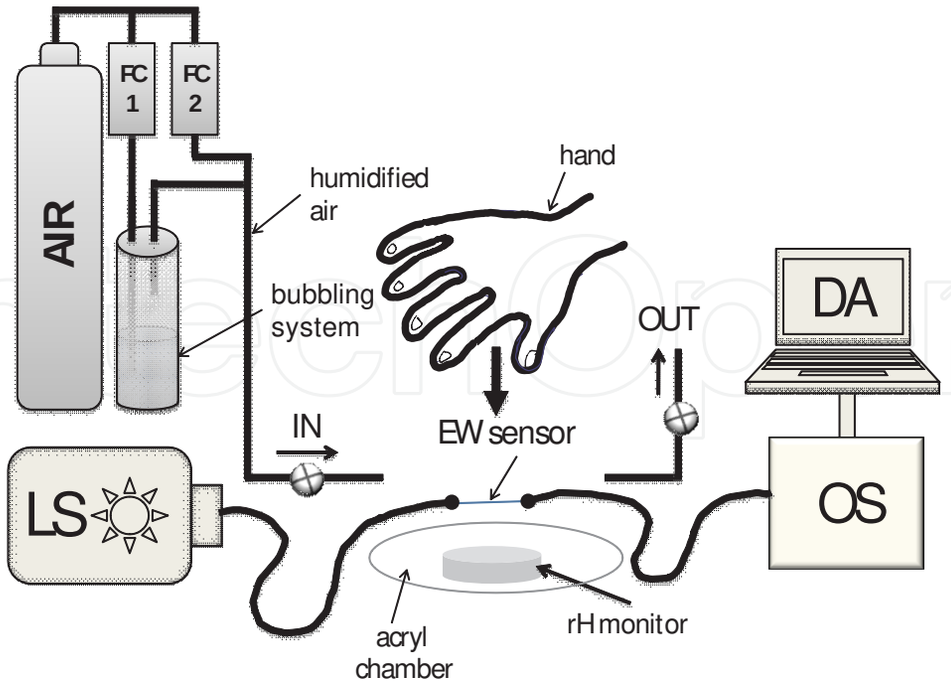

Figure 8. Experimental setup containing light source LS, optical spectrophotometer OS, data acquisition DA and humidified air generating system [54].

wavelengths). Measurements were conducted on the same day at similar conditions: the both participants were healthy, and hands were washed before the experiment with filtrated water. A slightly different response for two different people was observed. It should be noted that relative humidity level measured using a humidity logger, reached equilibrium at a maximum value of 95% within 1 min (data not shown). In general, relative humidity is an important factor that can influence sensor response. The sensor response to the skin gas emanations, however, is much slower as compared to the changes induced by relative humidity.

This difference in the senor response for two different participants suggests that some additional volatile compounds are exhaled by the human skin surface along increasing humidity. Interaction of compounds present in the skin gas with the PAH/TSPP film would contribute to the additional change observed in the output spectra.

From the complex sensor response observed over the wide spectral range, it is not a trivial task to discriminate the influences of humidity and skin gases. For the purpose of qualitative data description, the measured results were analyzed using principal component analysis (PCA, Statistical EXCEL add-in, V. 5.05 by Esumi Co. Ltd.) in order to reduce the multi-dimensionality of the obtained data. The 25 wavelengths at which the biggest intensity changes were observed were manually chosen from the difference spectra. Such selection was sufficient to obtain good separation between qualitatively different samples. The PCA results are shown in Figure 10, with a 96.5% cumulative proportion of PC1 and PC2. General observations are as follows: humidity points are grouped along the positive side of PC1 while most points representing responses to skin gas are located in the negative PC1 region. Additionally, PC2

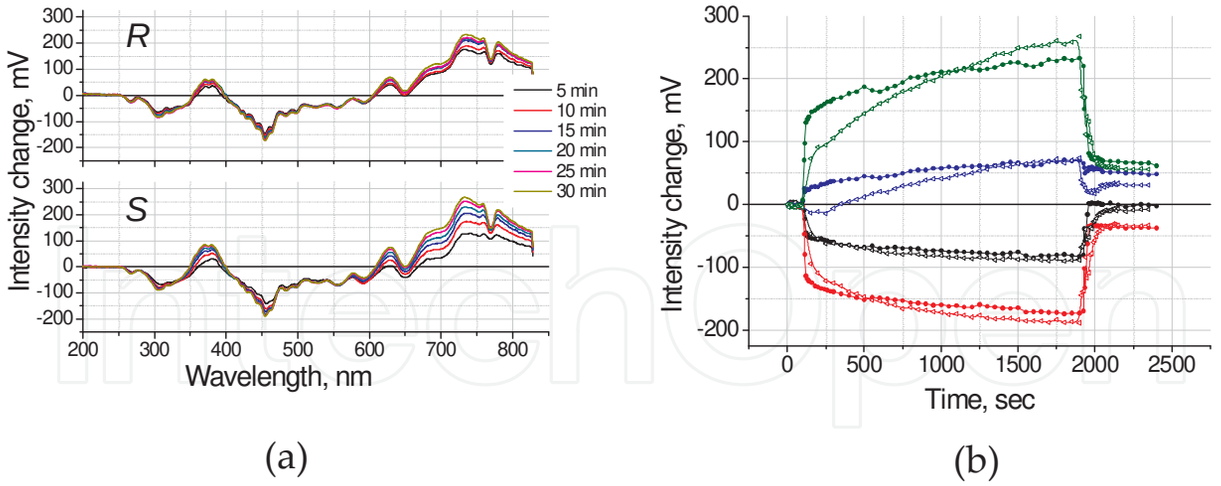

Figure 9. (a) Spectral changes induced by the skin gas emanations and (b) dynamic sensor response measured at selected wavelengths (black line 305 nm, red line 455 nm, blue line 629 nm, green line 733 nm) for different people (R-closed circles, S-open triangles).

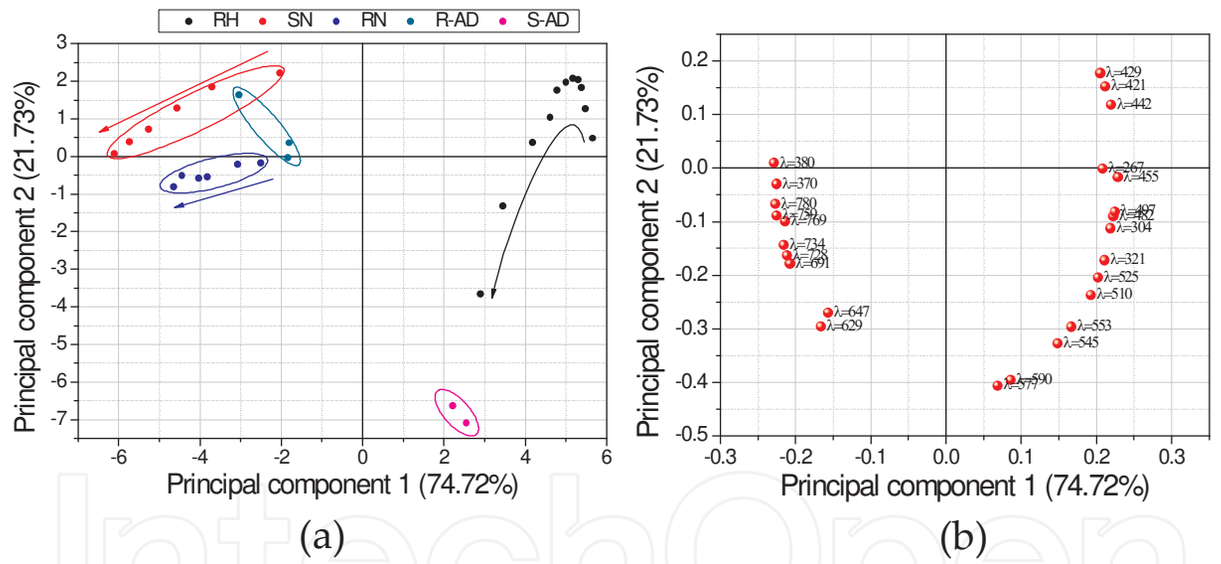

Figure 10. (a) Principal component analysis performed using the data measured at 25 wavelengths. Results measured at relative humidity change (black, with an arrow indicating increase of relative humidity values); Sensor response induced by skin gas emanations from participant R (blue, arrow indicating increase of sampling time of human skin gas emanation; i.e. attachment of the palm to the chamber containing the sensor, green point indicate the response one day after alcohol consumption); and from participant S (red, arrow indicating increase of sampling time of human skin gas emanation, magenta points show the response one day after alcohol consumption). (b) PCA loadings.

can possibly be used for the separation of participants who have different physiological conditions and different skin exhaling properties. The bigger distance between points in the S sample is probably related to the more intensive VOCs emanation. In addition, skin gasses were measured the day after alcohol consumption, and these points are added to the PCA plot.

http://dx.doi.org/10.5772/53399

Those measurements were repeated several times and skin gas sampling was done for 5 min. From the PCA plot, we can see that for the participant R, the points after consuming alcohol lie very close to those of the normal physiological conditions. For participant S, the points after consuming alcohol are located on the opposite side of the both principal component axes, which might be a result of a considerable change in the skin gas content after consuming alcohol. The obtained results further illustrate that the proposed sensor, combined with PCA data analysis, could recognize human samples and humidified air. However, based on the data gathered from only two persons, it is not possible to make a generalization on the behaviour of the sensor and on its ability to distinguish physiological conditions. We can speculate, however, that due to the normal physiological differences (for example in metabolic processes and related products excretion through the skin) between two people, the characteristics of the optical sensor response, such as response time and intensity change at different wavelengths, would be expected to be different. As shown in GC-MS and HPLC studies, variety of compounds can be found from human skin at normal conditions, such as ammonia [43], carbon monoxide [55], acetaldehyde [56], and acetone [42]. These compounds and many other emanations that are constituents of body odor are believed to contribute into the optical spectra of the EW sensor. Measurements using wider group of participants should be conducted, and the physiological condition of the various individuals tested should be considered to clarify the sensor response in more detail. Additionally, the response of the sensor to exposure to particular VOCs should be charcaterised to enable qualitative and quantitative analysis of skin gases.

3.2. Sensing based on tapered fibre optic sensors

A purpose-designed measurement chamber was used in order to characterise the tapered optical fibre sensor performance. The tapered section of the optical fibre, coated with the functional film, was inserted into the chamber. The desired gas concentrations were produced using a two-arm flow system described elsewhere [18]. The dry compressed air that was used as the carrier gas and ammonia gas of 100 ppm concentration were passed separately through two flowmeters. The two flows were combined to produce the desired ammonia concentration in the measurement chamber. The concentration could be controlled by adjusting the flow rates of the ammonia and of the air.

The transmission spectrum was recorded with a 1 Hz update rate as the device was exposed to a given ammonia concentration and subsequently flushed with dry air. The difference spectrum was plotted by subtracting a spectrum measured at a given ammonia concentration from the spectrum recorded in the presence of dry air. The baseline spectrum and sensor response of each experiment were recorded by passing dry air through the measurement chamber until the signal measured at a wavelength of 700 nm reached equilibrium.

The results are shown in Figure 11a–11d. As the ammonia concentration increased from 10 ppm up to 100 ppm, the intensity measured at 700 nm increased for the 10 μm and 12 μm diameter optical fibre tapers (Figure 11b). Interaction of the ammonia molecule with TSPP leads to the deprotonation of the pyrolle ring of TSPP and hence influences the electrostatic interaction between the TSPP moieties in the PAH/TSPP film [18, 39]. Consequently, the

biggest change in absorbance is observed at 700 nm (Q band), which may be closely related to the aggregation state of the TSPP molecules [20].

Interestingly, when measurements were conducted using the tapered fibres with 10 and 12 μm waist diameters, the channeled spectra did not exhibit a wavelength shift in response to exposure to ammonia, suggesting that ammonia–induced RI change cannot be measured with tapers of these diameters, possibly because the modes are tightly bound and the influence of the modes' evanescent field interaction with the coatings do not induce significant differential changes in the propagation constants (Figure 11b). When the 9 μm diameter tapered fibre coated with the $(PAH/TSPP)_5$ film was exposed to ammonia, a red–shift of the spectral features at 1000 and 1040 nm was observed that saturates with the increase of the concentration (Figure 11c). We can assume that the wavelength red–shift of the spectral features is caused by the ammonia–induced change in the RI of the PAH/TSPP film. It should be noted that this change is not continuous and saturation occurs between 0 and 50 ppm (Figure 11c). The 9 μm diameter tapered fibre possesses higher sensitivity to RI change as compared to 10 and 12 μm diameter tapered fibres. The absence of the intensity change at 700 nm can be explained by considering the transmission spectrum of the 9 μm diameter tapered fibre obtained after deposition of the 5th bilayer of the PAH/TSPP film (data not shown); the optical power at 700 nm transmitted to the spectrometer is very low, complicating the measurement of the small ammonia–induced intensity change. We can conclude from these results that the wavelength shift near 1000 μm observed in the transmission spectrum of the 9 μm diameter tapered fibre is sensitive to ammonia-induced RI changes of the coating and the change in transmitted power near 700 nm of the 10 and 12 μm tapered fibres can be used to monitor ammonia gas concentration.

Dynamic ammonia–induced changes of the tapered fibres with 10 and 12 μm waist diameters coated with the $(PAH/TSPP)_5$ film were monitored at 700 nm, as shown in Figure 11d. The measurement principle for these waist diameters is based on evanescent wave spectroscopy. The response time and recovery time (t_{90}) of the sensor to increasing ammonia concentration were within 100 sec and 240 sec, respectively. The sensitivity of the device derived from the slope of the calibration curve is 0.440±0.002 mV/ppm and estimated limit of detection (*LOD*) calculated using the 3σ method is 2±0.3 ppm (inset of Fig. 11d). It should be noted that sensitivity of the proposed sensor is ca. 3 times higher as compared to the PDDA/TSPP film assembled onto the quartz substrate (Korposh 2006). This is most plausibly a result of the higher localized energy at the tapered region of the optical fibre and thus increased efficiency of the interaction between the probe light and the functional film. On the other hand, the sensitivity of the fabricated device was ca. 6 times lower than that of a multimode optical fibre coated with the PDDA/TSPP film [18]. This can be attributed to the presence of TSPP in *J*-aggregated form in higher concentration in the PDDA/TSPP film as compared to the PAH/TSPP film used in this study. However, the presence of TSPP in different forms inside the PAH film may allow the coating to exhibit sensitivity to different chemical compounds, thus increasing the application range of the proposed sensor. This hypothesis will be thoroughly explored in the future work. In addition, the tapered fibre may operate as both an evanescent wave spectroscope and as a refractometer. Thus, in contrast to solely evanescent wave spectroscopy, materials without absorbance features in the UV-vis range may be employed as

http://dx.doi.org/10.5772/53399

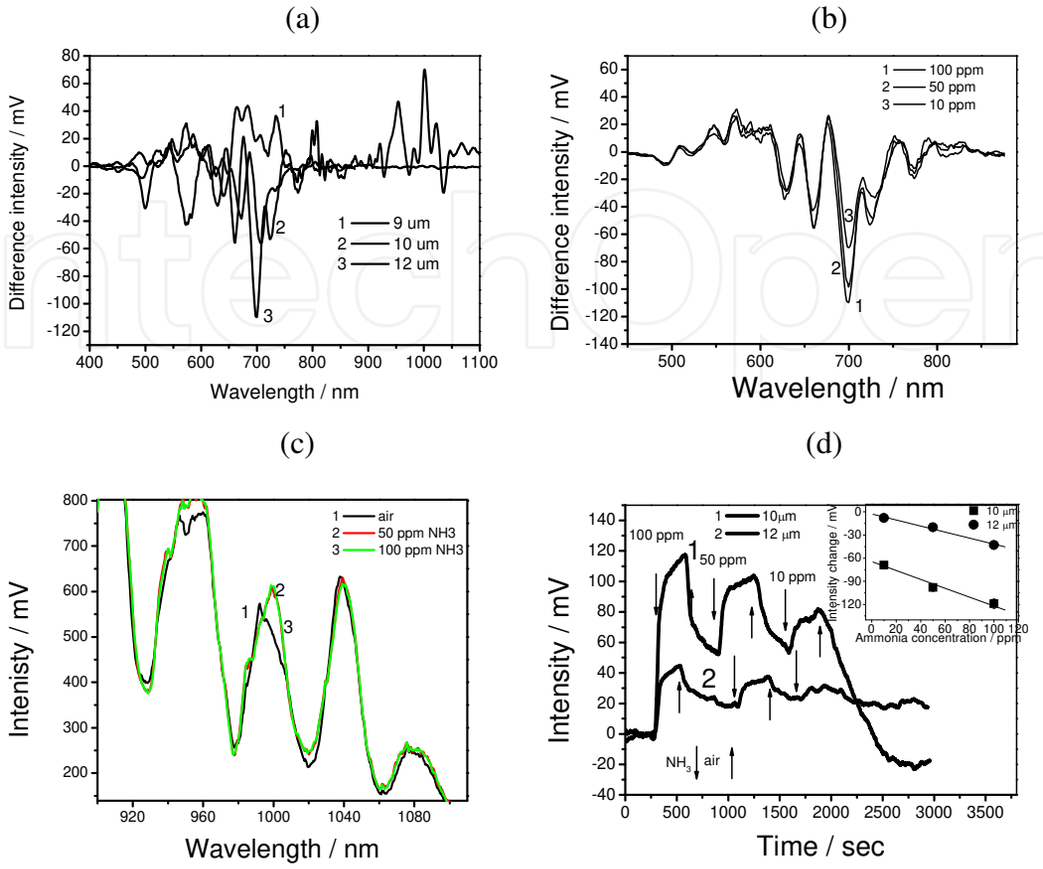

Figure 11. (a) Transmission difference spectra obtained by subtracting a spectrum measured in the 100 ppm ammonia atmosphere from the spectrum measured in air with the tapered fibres of 9, 10, and 12 μm diameter modified with a $(PAH/TSPP)_5$ film, (b) transmission difference spectra of the 10 μm tapered fibre measured at given ammonia concentrations from 10 to 100 ppm, (c) transmission spectra of the 9 μm tapered fibre measured before and after 50 and 100 ppm ammonia exposures, and (d) dynamic responses of the 10 and 12 μm diameter tapered fibres to the varying ammonia concentration (from 100 ppm to 10 ppm) recorded at 706 nm, where arrows indicate the admission time of ammonia and air into the measurement chamber. The inset of Figure 11(d) shows a calibration curve plotted from the difference spectra data taken at 706 nm: squares and circles show the data of the 10 and 12 μm diameter tapered fibres, respectively.

sensitive layers, extending the utility of the chemical fibre optic sensors and the class of the detectable analytes.

The fabricated device was exposed to varying relative humidity to study its effect on the sensor response. When rH was reduced from 70 % to 10% and increased back to 70%, no significant change in the transmission spectra was observed (Figures 12a and 12b) revealing selectivity of the sensor to ammonia over rH. The immunity of the sensor to rH change is very important for real-world practical applications where humidity is one of the major interfering parameters. For example, ammonia detection in breath is highly important non-invasive diagnostic tool in medicine [37], but highly challenging due to the high humidity present in breath. To-date, to the best of our knowledge, there is no sensor with satisfactory sensitivity and selectivity for

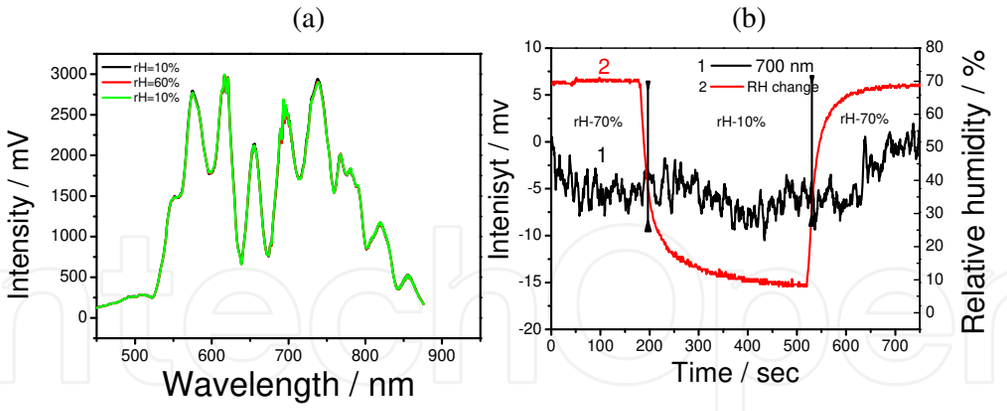

Figure 12. (a) Transmission spectra of the 10 μm diameter tapered fibre modified with a 5-cycle PAH/TSPP film measured before and after change of the relative humidity and (b) dynamic responses of the 10 μm diameter tapered fibre to the varying RH from 70 to 10 % and backwards recorded at 706 nm, where lines indicate the admission time of dry air into the measurement chamber; line 1, sensor response; and line 2, RH change measured using humidity logger.

the detection of ammonia in breath. In our future study of the use of this sensor for ammonia breath measurement, the cross-sensitivity to other gases will be investigated.

3.3. Sensing based on LPG fibre optic sensors

The sensitivity to ammonia in water of an LPG coated with a $(PDDA/SiO_2)_{10}$ film that was infused with TSPP was characterized by sequential immersion of the coated LPG into ammonia solutions with different concentrations (0.1, 1, 5 and 10 ppm). The lower ammonia concentrations were prepared by dilution of the stock solution of 28 wt%. In order to assess the stability of the base line, the coated LPG was immersed several times into 150 μL of pure water. The decrease of attenuation of the second resonance band, LP_{021}, at 800 nm, indicates the partial removal of the adsorbed TSPP molecules. The equilibrium state was achieved after several exposures into water. For the ammonia detection, the LPG fibre was exposed into a 150 μL ammonia solution of 0.1 ppm, followed by drying and immersion into ammonia solutions of 1, 5 and 10 ppm.

The response of the transmission spectrum to varying concentration of ammonia is shown in Figure 13a. The dynamic response of the sensor was assessed by monitoring the transmission at the centre of the LP_{021} resonance band at 800 nm. The response is shown in Figure 13b, where "air" region and "H_2O" and "NH_3" regions correspond to the transmission recorded at 800 nm after drying the LPG and immersing the device into water and ammonium solutions, respectively. After repeating the process of immersion in water and drying 4 times, the recorded spectrum was stable, demonstrating the robustness and stability of the employed molecules in aqueous environments (H_2O regions indicated in Figure 13). On immersion in 1 ppm and 5 ppm ammonia solutions, the transmission measured at 800 nm increases. The transmission when the coated LPG was immersed in a 10 ppm ammonia solution exhibits a further increase, reaching a steady state within 100 s, as shown in Figure 13b. The resonance feature corresponding to coupling to the LP_{020} cladding mode exhibits additional small red shifts of 0.5 and

http://dx.doi.org/10.5772/53399

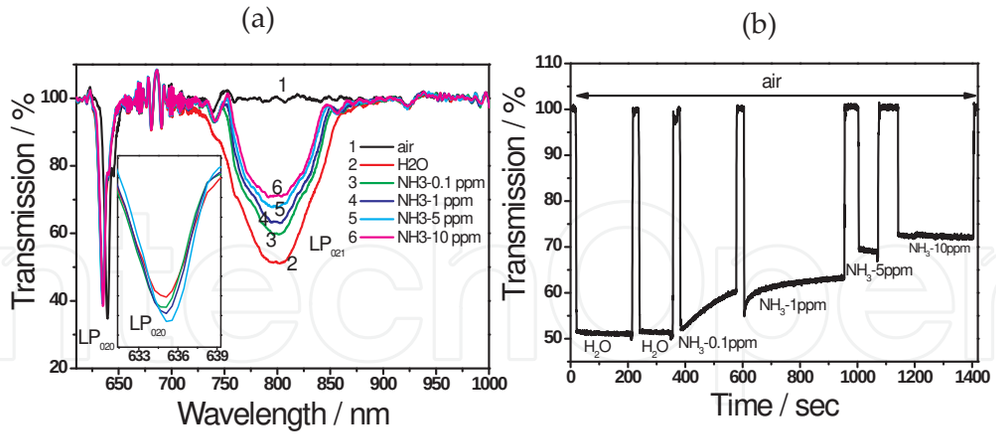

Figure 13. (a) Transmission spectra of the LPG coated with a TSPP infused $(PDDA/SiO_2)_{10}$ film due to immersion into water and into ammonia solutions of different concentrations: "H_2O", LPG exposed into water; "air", LPG in air after drying with N_2 gas; "NH_3 x ppm", LPG exposed into a x ppm ammonia solution, where x = 0.1, 1, 5 and 10. (b) Dynamic response to water and ammonia solutions (0.1, 1, 5 and 10 ppm) recorded at 800 nm; LP_{020} and LP_{021} are labelling the linear polarized 020 and 021 modes, respectively.

1.5 nm when subsequently immersed in solutions of 1 ppm and 10 ppm ammonia concentration, respectively, along with decreases in amplitude, as shown in Figure 13a. The limit of detection (LOD) for the 100 μm period LPG coated with a $(PDDA/SiO_2)_{10}$ film that was infused with TSPP was 0.14 ppm and 2.5 ppm when transmission and wavelength shift were measured respectively. The LOD was derived from the calibration curve and the using equation 3 [40].

Response of the sensor to ammonia gas was measured with ammonia vapor of different concentrations generated from aqueous ammonia solutions in proximity to the modified LPG sensor. Ammonia gas was generated by placing 100 μl of aqueous ammonia solution with different concentrations into the measurement chamber. Concentrations of ammonia in the gas phase were measured using ammonia detection gas tubes (GasTec, Japan) and compared with the values of the corresponding solutions. The sensor response was recorded with a resolution of 1 Hz.

The transmission spectrum was recorded with each analyte solution present in the chamber before and after its removal. To regenerate the sensor response the optical fibre was washed with water and flashed using nitrogen gas.

A linear increase in the separation of the 1st and 2nd bands in the TS was observed at the exposure of the LPG coated with the PDDA/PAA to the increasing ammonia gas concentration, Figures 15a and 15b. The sensitivity of the sensor was estimated to be 0.35 and 0.31 nm/ppm for the 1st and 2nd resonance bands, respectively (Figure 15b). The limit of detection (LOD) for both resonance bands was estimated to be 1.6 and 2.3 ppm ($3\sigma = 0.47$ nm), respectively. The sensor response was fast and almost saturated within 5 min. Along with the wavelength shift, both the extinction of both of the resonance bands also decreased in proportion to the increase

of the ammonia gas concentration. Moreover, the sensor response could be easily regenerated by washing the LPG sensor with water (data not shown).

To confirm the selectivity of the sensor, different analyte gases of amine and non-amine compounds were tested (see Figure 15c). The sensor demonstrated higher sensitivity towards amine compounds. It appears that the superior binding of the sensor to amine compounds is assigned to the acid-base reaction between the functional moieties of PAA and the amine compounds. Other parameters of the analytes such as molecular size, solubility to the film, and equilibrium constant (pK_a or pK_b) can be significant factors to determine the selectivity and additional examination is in progress.

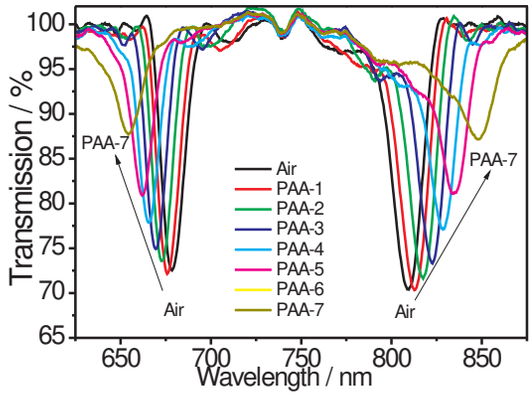

Figure 14. TS changes of the LPG fibre after deposition of PAA.

In order to demonstrate the capabilities and versatility of the coated optical fibre LPG in chemical sensing, a PAH/SiO_2 film was deposited onto the surface for the detection of the organic compounds, namely aromatic carboxylic acids (ACAs, see Scheme 2). The LbL procedure described above was employed for coating the LPG.

After deposition of the PAH/SiO_2 film onto the LPG it was exposed to aqueous solutions of ACAs in the range of 0.001–1000 μM of individual ACAs or their mixtures. All experiments were conducted using the same sensor transducer. After exposure and measurement, the substrate was washed in 0.1 wt% of aqueous ammonia in order to remove adsorbed analytes from the PAH/SiO_2 film.

For the detection of the chemical binding the LPG coated with the $(PAH/SiO_2)_{10}$ film was exposed to different ACAs of concentration 10 μM in water, which lead to a significant change in the TS, Figure 17a. The magnitude of the TS change at 825 nm differed according to the number of carboxylic acid groups in the molecule, the molecular weights and the pKa values of the ACAs. The largest change was observed when the coated LPG was exposed to mellitic acid (MA), as shown in Figures 16a and 16b. As MA has the biggest molecular weight and the highest number of the functional group, suggesting the efficient binding to the amino functional groups of PAH. The response of phthalic acid (PA) is higher than that of BA. These

http://dx.doi.org/10.5772/53399

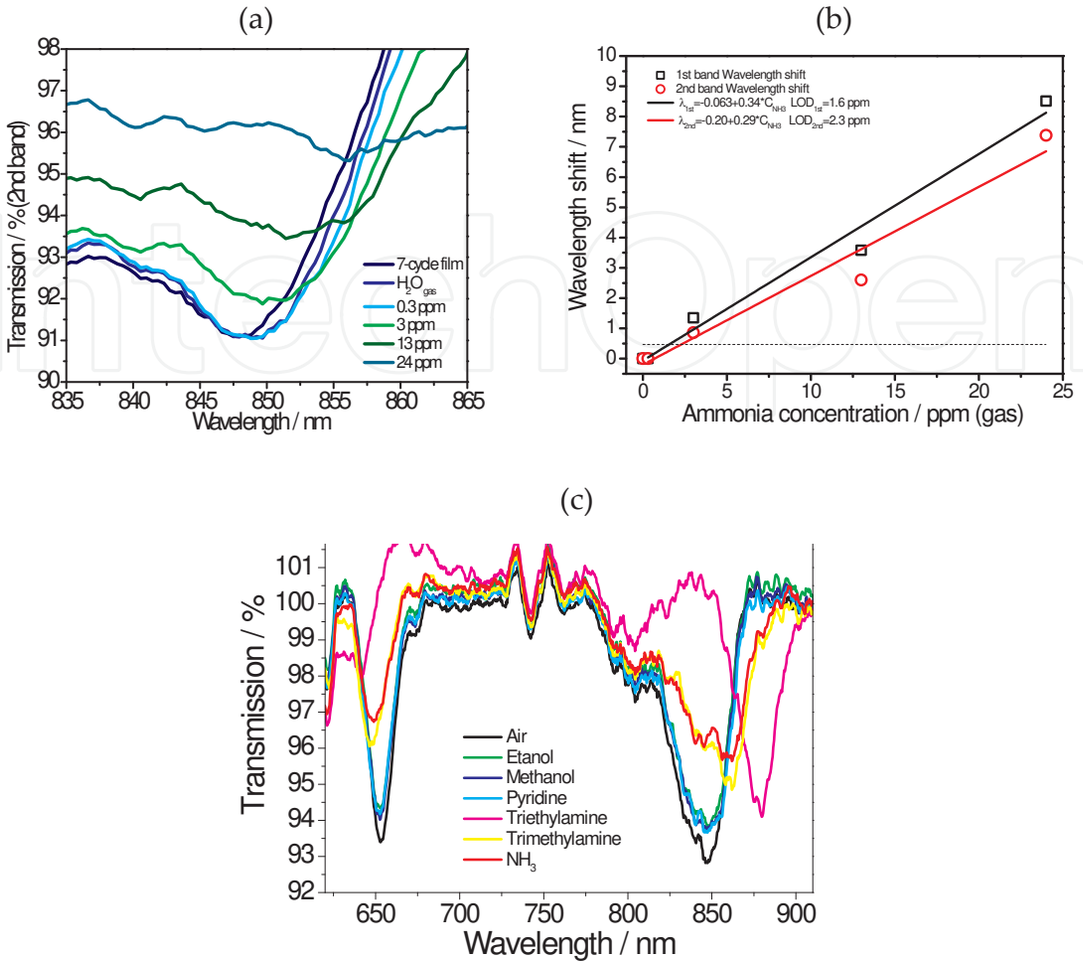

Figure 15. (a) TS changes of the 2nd resonance band of the LPG fibre with a 7-cycle PDDA/PAA film at the exposure to different concentrations of ammonia gas. (b) Ammonia concentration dependence of the 7-cycle PDDA/PAA film coated LPG fibre on wavelength shifts at 654 and 848 nm. (c) TS changes of the LPG fibre modified with a 7-cycle PDDA/PAA film at the exposure to 100 ppm ammonia gas (estimated from the calibration curve of Figure 15b) and to saturated amine and non-amine gases.

results suggest that the sensitivity of the sensor depends additionally on the number of the functional group and increases in the order of MA >> PA > BA (Figures 16a and 16b). It should be noted that, when MA binds to the PAH, the sensor response cannot be regenerated simply by water washing (see "H_2O" after MA exposure in Figure 17b). The sensor response can be perfectly recovered, however, using 0.1 wt% NH_3 aqueous solution for 10 min (see areas marked with "*" in Figures 16b and 16c).

The adsorption of the ACAs in the PAH/SiO_2 film can be described using a Langmuir adsorption curve. The calculated binding constant of BA to the PAH/SiO_2 film is estimated to be 1.36 ± 0.01×10^6 M^{-1}. The lowest measurable concentration was 1 nM when MA was used, with a binding constant of 5.6 ± 0.01×10^8 M^{-1}

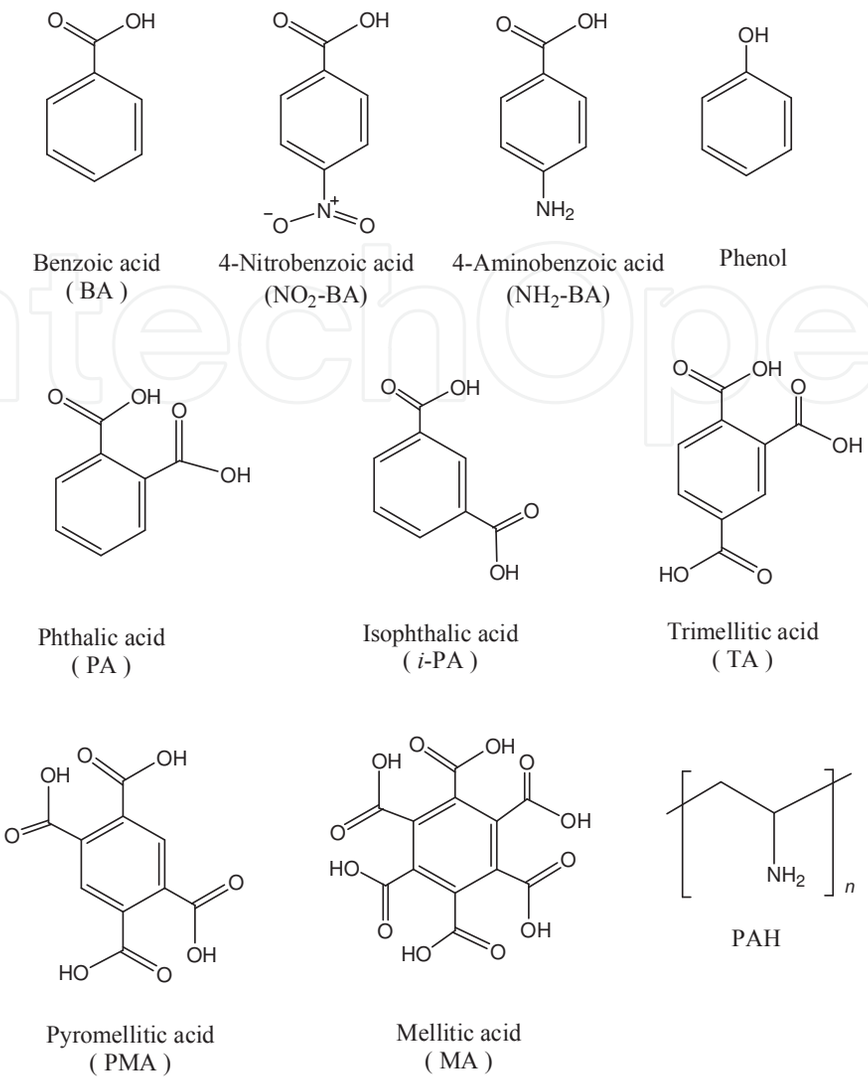

Scheme 2. Structures of ACAs used for binding test and cationic polymer (PAH) used for film assembly.

4. Summary

In summary, in this chapter fibre-optic sensors based on different measurement principles were coated with the nano-assembled thin films for the detection of various chemical compounds. When of the different fibre optic sensor designs were characterised for their response to ammonia gas, the highest sensitivity was observed when EWFOS was coated with the porphyrin based film, showing an LOD of 0.9 ppm. The coated LPG had an LOD of 1.6 ppm and the tapered fibre has an LOD of 2 ppm. The high sensitivity of the EWFOS makes it a promising device for medical applications where there is a requirement of measure low concentrations of specific chemical compounds. The possibility of employing EWFOS for medical diagnosis was explored in the example of skin emanation measurements. In solution, the LOD of LPG sensor was as low as 0.14 ppm for ammonia and the lowest measurable concentration for mellitic acid was 1 nM. From a practical point of view, the EWFOS are limited

http://dx.doi.org/10.5772/53399

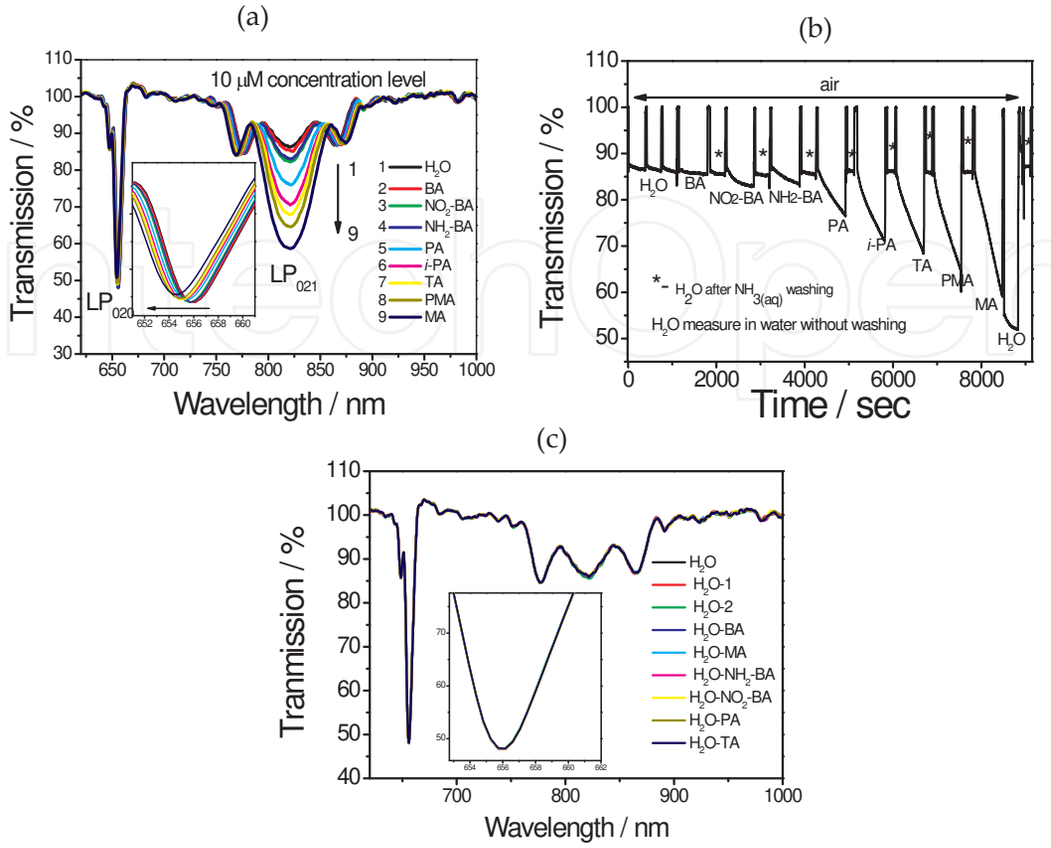

Figure 16. (a) Evolution of the transmission spectra due to the exposure of the optical fibre LPG coated with a $(PAH/SiO_2)_{10}$ film to 10 μM of different ACAs and (b) time-dependence of the transmission measured at 825 nm; "air" arrow indicates signal measured in air, corresponding to spectra 1 in Figure 16a. (c) Transmission spectra measured in water after exposure to ACAs and washing step using NH_3 (aq); inset shows magnified LP_{020} resonance band.

to the materials with the strong absorption features, while tapered and LPGs fibres can be modified with the wider class of materials, including transparent materials. In addition, tapered and LPGs fibres offer wavelength-encoded information, which overcomes the referencing issues associated with intensity based approaches. Moreover, LPGs owing to the multiplexing capabilities enable sensor design for multi-analyte detection using a single optical fibre. Our future work will focus on the creation of multi-analyte detection systems in which the number of individual gratings with the characteristic grating period inscribed in the single optical fibre will be chemically modified for sensitive detection of targeted analytes.

Acknowledgements

This work was supported by the Regional Innovation Cluster Program of the Ministry of Education, Culture, Sports, Science and Technology (MEXT), Japan. The authors from

Cranfield are grateful to the Engineering and Physical Sciences Research Council, EPSRC, UK for funding under grants EP/D506654/1 and GR/T09149/01.

Author details

Sergiy Korposh[1], Stephen James[2], Ralph Tatam[2] and Seung-Woo Lee[1*]

*Address all correspondence to: leesw@kitakyu-u.ac.jp

1 Graduate School of Environmental Engineering, the University of Kitakyushu, Kitakyushu, Japan

2 School of Engineering, Cranfield University, Cranfield, UK

References

[1] Seifert, B, Englert, N, Sagunski, H, & Witten, J. Guidline values for indoor air pollutants. Proc. 8th Int. Con. on Indoor Air Quality and Climate (1999). Indoor Air, Edinburgh, Scotland, 1999) 499.

[2] Natale, C D, Macagnano, A, Martinelli, E, Paolesse, R, Arcangelo, D, Roscioni, G, Finazzi-agrò, C, & Amico, A, D. A. Lung cancer identification by the analysis of breath by means of an array of non-selective gas sensors. Biosens. Bioelectron. (2003). , 18-1209.

[3] Takahara, N, Yang, D-H, Ju, M-J, Hayashi, K, Toko, K, Lee, S-W, & Kunitake, T. Anchoring of cyclodextrin units on TiO2 thin layer for effective detection of nitro-aromatics: A novel electrochemical approach for landmine detection. Chem. Lett. (2006). , 35-1340.

[4] Grattan, K. T. V, & Meggitt, B. T. (1999). Chemical and environmental sensing, Dordrecht, Boston : Kluwer

[5] Bucholtz, F, Dagenais, D M, & Koo, K P. High frequency fibre-optic magnetometer with 70 fT per square root hertz resolution. Electronics Letters (1989). , 25(25), 1719-1721.

[6] Dandridge, A. Fibre optic sensors based on the Mach-Zehnder and Michelson interferometers, In: Fiber Optic Sensors: An Introduction for Engineers and Scientists, edited by E. Udd. New York: Wiley (1991).

[7] Yuan, L, & Yang, J. Two-loop based low-coherence multiplexing fibre optic sensors network with Michelson optical path demodulator, Proceedings of 17th International Conference on Optical Fibre Sensors (2005). , 595-598.

[8] Russell, S J, & Dakin, J P. Location of time-varying strain disturbances over a 40 km fibre section, using a dual-Sagnac interferometer with a single source and detector. Proceedings of 13th International Conference on Optical Fibre Sensors (1999). , 580-584.

[9] Rao, Y J, Cooper, M R, Jackson, D A, Pannell, C N, & Reekie, L. High resolution static strain measurement using an in-fibre-Bragg-grating-based Fabry Perot sensor. Proceedings of 14th International Conference on Optical Fibre Sensors (2000). , 284-287.

[10] Cibu, a E, & Donlagic, D. All-fibre Fabry-Perot strain sensor. Proceedings of 2nd European Workshop on OFS (2004). , 180-183.

[11] Lin, C-J, Tseng, Y-T, Lin, S-C, Yang, C-S, & Tseng, F-G. A novel in-vitro and in-situ immunoassay biosensor based on fibre-optic Fabry-Perot interferometry. Proceedings of 2nd European Workshop on Optical Fibre Sensors (2004). , 304-307.

[12] Leung, A, Rijal, K, Shankar, P M, & Mutharasan, R. Effects of geometry on transmission and sensing potential of tapered fibre sensors. Biosensors and Bioelectronics (2006). , 21(12), 2202-2209.

[13] Vohra, S T, Todd, M D, Johnson, G A, Chang, C C, & Danver, B. A. Fibre Bragg grating sensor system for civil structure monitoring: applications and field tests, Proceedings of 13th International Conference on Optical Fibre Sensors (1999). , 32-37.

[14] Schroeder, R J, Yamate, T, & Udd, E. High pressure and temperature sensing for the oil industry using fiber Bragg gratings written onto side hole single mode fiber. Proceedings of 13th International Conference on Optical Fibre Sensors (1999). , 42-45.

[15] Corres, J, Arregui, F, & Matías, I. Sensitivity optimization of tapered optical fiber humidity sensors by means of tuning the thickness of nanostructured sensitive coatings. Sens. and Act. B. (2007). , 122-442.

[16] Leung, A, Shankar, P, & Mutharasan, R. Real-time monitoring of bovine serum albumin at femtogram/mL levels on antibody-immobilized tapered fibers. Sen. and Act.B. (2007). , 123-888.

[17] James, S, & Tatam, R. Fibre optic sensors with nano-structured coatings. J. Opt. A: Pure Appl. Opt. (2006). S430.

[18] Korposh, S, Kodaira, S, Lee, S-W, Batty, W J, & James, S W. Nano-assembled thin film gas sensor. II. An intrinsic high sensitive fibre optic sensor for ammonia detection. Sensor and Materials (2009). , 21(4), 179-189.

[19] Ariga, K, Lvov, Y, & Kunitake, T. Assembling alternate dye-polyion molecular films by electrostatic layer-by-layer adsorption. Journal of American Chemical Society, (1997). , 119(9), 2224-2231.

[20] Takagi, S, Eguchi, M, Tryk, D A, & Inoue, H. Porphyrin photochemistry in inorganic/organic hybrid materials: Clays, layered semiconductors, nanotubes, and mesoporous materials. J. Photochem. Photob. C: Photochem. Rev. (2006).

[21] Kadish, K M, Smith, K M, & Guilard, . . The Porphyrin Handbook, Academic Press, ISBN 0123932009, San-Diego 2007.

[22] Schick, G A, Schreiman, I C, Wagner, R W, Lindsey, J S, & Bocian, D F. Spectroscopic characterization of porphyrin monolayer assemblies. Journal of American Chemical Society, (1989). 1520-5126, 1520-5126.

[23] Jarzebinska, R, Cheung, C S, James, S W, & Tatam, R P. Response of the transmission spectrum of tapered optical fibres to the deposition of a nanostructured coating. Meas. Sci. Technol. (2009). pp).

[24] Jarzebinska, R, Korposh, S, James, S, Batty, W, Tatam, R, & Lee, S. W. Optical gas sensor fabrication based on porphyrin-anchored electrostatic self-assembly onto tapered optical fibres. Analytical Letters. (2012). , 45-1297.

[25] Corres, J M, Matias, I R, Bravo, J, & Arregui, F. G. Tapered optical fiber biosensor for the detection of anti-gliadin antibodies. Sen. and Act.B. (2008). , 135-608.

[26] Bhatia, V, & Vengsarkar, V. A M. Optical fibre long-period grating sensors. Optics Letters(1996). , 21-692.

[27] Korposh, S, James, S W, Lee, S-W, Topliss, S M, Cheung, S C, Batty, W J, & Tatam, R P. Fiber optic long period grating sensors with a nanoasembledmesoporous film of SiO2 nanoparticles. Optics Express (2010). , 18(12), 13227-13238.

[28] Shi, Q, & Kuhlmey, B T. Optimization of photonic bandgap fiber long period grating refractive-index sensors. Optics Communications (2009). , 282-4723.

[29] Patrick, H, Kersey, A, & Bucholtz, F. Analysis of the response of long period fiber gratings to external index of refraction. J. Lightwave Technol. (1998). , 16-1606.

[30] Korposh, S, Selyanchyn, R, Yasukochi, W, Lee, S-W, James, S, & Tatam, R. Optical fibre long period grating with a nanoporous coating formed from silica nanoparticles for ammonia sensing in water. Materials Chemistry and Physics (2012). , 133-784.

[31] Korposh, S, Wang, T, James, S, Tatam, R, & Lee, S-W. Pronounced aromatic carboxylic acid detection using a layer-by-layer mesoporous coating on optical fibre long period grating. Sensors and Actuators B: Chemical(2012). in press.

[32] Ye, C C, James, S W, & Tatam, R P. Simultaneous temperature and bend sensing with long-period fiber gratings. Optics Letters (2000). , 25-1007.

[33] Cheung, S C, Topliss, S M, James, S W, & Tatam, R P. Response of fibre optic long period gratings operating near the phase matching turning point to the deposition of nano-structured coatings. J. Opt. Soc. Am. B (2008). , 25-897.

[34] Wang, T, Korposh, S, Wong, R, James, S, Tatam, R, & Lee, S. W. A novel ammonia gas sensing using a nanoassembled polyelectrolyte thin film on fiber optic long period gratings.Chemistry Letters (2012). in press.

[35] Lee, S-W, Takahara, N, Korposh, S, Yang, D-H, Toko, K, & Kunitake, T. Nanoassembled thin film gas sensors. III. Sensitive detection of amine odors using TiO2/ Poly(acrylic

acid) ultrathin film quartz crystal microbalance sensors. Analytical Chemistry (2010). , 822228-2236.

[36] Timmer, B, & Olthuis, W. Van den Berg A. Ammonia sensors and their applications-a review. Sens. Actuators B, (2005). , 107-666.

[37] Turner, C, Španel, P, & Smith, D. A longitudinal study of ammonia, acetone and propanol in the exhaled breath of 30 subjects using selected ion flow tube mass spectrometry, SIFT-MS. Physiol. Meas. (2006). , 27-321.

[38] Gregory van Patten PShreve A P, Donohoe R J. Structural and photophysical properties of a water-soluble porphyrin associated with polycations in solutions and electrostatically-assembled ultrathin films. Journal of Physical Chemistry:B (2000). , 104(25), 5986-5992.

[39] Korposh, S O, Takahara, N, Ramsden, J J, Lee, S-W, & Kunitake, T. Nano-assembled thin film gas sensors. I. Ammonia detection by a porphyrin-based multilayer film. Journal of Biological Physics and Chemistry (2006). , 6-125.

[40] Swartz, M E, & Krull, I S. Analytical Method Development and Validation, Marcel Dekker, Inc.: NY USA; (1997).

[41] Ohira, S I, & Toda, K. Micro gas analyzers for environmental and medical applications. Anal. Chim.Acta (2008). , 619-143.

[42] Yamane, N, Tsuda, T, Nose, K, Yamamoto, A, Ishiguro, H, & Kondo, T. Relationship between skin acetone and blood beta-hydroxybutyrate concentrations in diabetes. Clin. Chim. Acta, (2006). , 365-325.

[43] Nose, K, Mizuno, T, Yamane, N, Kondo, T, Ohtani, H, Araki, S, & Tsuda, T. Identification of ammonia in gas emanated from human skin and its correlation with that in blood. Anal. Sci. (2005). , 21-1471.

[44] Nose, K, Nunome, Y, Kondo, T, Araki, S, & Tsuda, T. Identification of gas emanated from human skin: methane, ethylene, and ethane, Anal. Sci. (2005). , 21-625.

[45] Akiyama, A, Imai, K, Ishida, S, Ito, K, Kobayashi, T, Nakamura, H, Nose, K, & Tsuda, T. Determination of aromatic compounds in exhalated from human skin by solid-phase micro extraction and GC/MS with thermo desorption system. Bunseki Kagaku (2006). , 55-787.

[46] Penn, D J, Oberzaucher, E, Grammer, K, Fischer, G, Soini, H A, Wiesler, D, Novotny, M V, Dixon, S. J, Xu, Y, & Brereton, R G. Individual and gender fingerprints in human body odour. J. R. Soc. Interface, (2007). , 4-331.

[47] Turner, A, & Magan, F. N. Electronic noses and disease diagnostics. Nat. Rev. Microbiol., (2004). , 2(2), 160-166.

[48] Pavlou, A K, Magan, N, Jones, J M, Brown, J, Klatser, P, & Turner, A. P F. Detection of Mycobacterium tuberculosis (TB) in vitro and in situ using an electronic nose in combination with a neural network system. Biosens. Bioelectron. (2004). , 20-538.

[49] Kodogiannis, V, & Wadge, E. The use of gas-sensor arrays to diagnose urinary tract infections. Int. J. of Neur. Syst. (2005). , 15-363.

[50] Dalton, P, Gelperin, A, & Preti, G. Volatile metabolic monitoring of glycemic status in diabetes using electronic olfaction. Diabetes Technol. The. (2004). , 6(4), 534-544.

[51] Voss, A, Baier, V, Reisch, R, Von Roda, K, Elsner, P, Ahlers, H, & Stein, G. Smelling renal dysfunction via electronic nose. Ann. Biomed. Eng. (2005). , 33(5), 656-660.

[52] Haick, H, Hakim, M, Patrascua, M, Levenberg, C, Shehada, N, Nakhoul, F, & Abassi, Z. Sniffing chronic renal failure in rat models via an array of random network of single-walled carbon nanotubes. ACS Nano (2009). , 3(5), 1258-1266.

[53] Peng, G, Tisch, U, Adams, U, Hakim, M, Shehada, N, Billan, S, Abdah-bortnyak, R, Kuten, A, & Haick, H. Diagnosing lung cancer in exhaled breath using gold nanoparticles. Nat. Nanotechnol. (2009). , 4(10), 669-673.

[54] Selyanchyn, R, Korposh, S, Yasukochi, W, & Lee, S. W. A preliminary test for skin gas assessment using a porphyrin based evanescent wave optical fiber sensor. Sensors & Transducers Journal (2011). , 125(2), 54-67.

[55] Nose, K, Ueda, H, Ohkuwa, T, Kondo, T, Araki, S, Ohtani, H, & Tsuda, T. Identification and assessment of carbon monoxide in gas emanated from human skin. Chromatography (2006). , 27-63.

[56] Sekine, Y, Toyooka, S, & Watts, S F. Determination of acetaldehyde and acetone emanating from human skin using a passive flux sampler- HPLC system. J. Chromat. B (2007). , 859-201.